Available online at www.sciencedirect.com
SCIENCE DIRECT
Polymer 47 (2006) 4026–4035
polymer
www.elsevier.com/locate/polymer

Structure–property–performance relationships of sulfonated poly(arylene ether sulfone)s as a polymer electrolyte for fuel cell applications

Yu Seung Kim [a], Brian Einsla [b], Mehmet Sankir [b], William Harrison [b], Bryan S. Pivovar [a,*]

[a] *Electronic and Electrochemical Materials and Devices, MST-11, MS-D429, Los Alamos National Laboratory, Los Alamos, NM 87545, USA*
[b] *Department of Chemistry and Materials Research Institute, Virginia Polytechnic Institute and State University, Blacksburg, VA 24061, USA*

Available online 7 March 2006

Abstract

This article focuses on structure–property–performance relationships of directly copolymerized sulfonated polysulfone polymer electrolyte membranes. The chemical structure of the bisphenol-based disulfonated polysulfones was systematically alternated by introducing fluorine moieties or other polar functional groups such as benzonitrile or phenyl phosphine oxide in the copolymer backbone. Ac impedance measurements of the polymer electrolyte membranes indicated that fluorine incorporation increased proton conductivity, while polar functional group incorporation decreased conductivity. Likewise, other properties such as water uptake and ion exchange capacity are impacted by the incorporation of fluorine moiety or polar groups. These properties are critically tied with H_2/air and direct methanol fuel cell performance. We have rationalized fuel cell performance of these selected copolymers in light of structure–property relationships, which gives useful insight for the development and application of next generation polymer electrolytes.

Keywords: Poly(arylene ether sulfone); Polymer electrolyte membrane; Proton conductivity

1. Introduction

During the last two decades, extensive efforts have been made to develop alternative hydrocarbon-based polymer electrolyte membranes in order to overcome the drawbacks of the current widely used perfluorosulfonic acid Nafion [1–3]. However, structure–property–performance relationships for hydrocarbon-based polymer electrolyte membranes (PEMs) have remained relatively unstudied. The lack of understanding in this area stems not only from insufficient data for alternative polymer electrolytes, but also due to difficulties in interpreting cross-influencing properties, such as ion exchange capacity (IEC), water uptake, morphology, acidity of sulfonic acid group, etc. Nevertheless, a few attempts have been made from limited experimental variations. Most established structure–property relationships of hydrocarbon-based PEMs are based on the effects of IEC (or relatedly, degree of sulfonation or equivalent weight). Several literature references have reported that the proton conductivity, methanol permeability and water swelling within a family of copolymers were found to be proportional to the IEC and often observed an abrupt increase at some specific IEC where a percolation limit occurred [4–6]. Cross-linking has also been investigated as a factor that influences structure–property relationships. Kerres and his co workers reported that (either covalent or ionic) crosslinked copolymers showed significantly reduced water swelling behavior without significant proton-conductivity loss [7,8]. Additional structural effects include bulkiness of polymer components and backbone stiffness. The independent research groups of Litt and Watanabe reported that polyimide membranes having bulky functional group (increased free volume) exhibited higher proton conductivity, particularly under low humidity conditions [9,10]. The work of Guiver [11] and our own [12] research group, on the other hand, showed that more rigid backbones restricted proton/methanol transport and water swelling. For example, rigid polyimide produced higher barrier properties than flexible polyimide or polysulfone membranes. These examples represent a few studies that investigate structure–property relationships in PEMs; however, the factors influencing structure–property relationships have been limited to a very narrow range of variables and these properties have not been extended to the interpretation of observed fuel cell performance.

In this paper we extend the study of structure–property relationships by examining chemical and structural effects of different chemical structural variations on hydrocarbon based

* Corresponding author. Tel.: +1 505 665 8918; fax: +1 505 665 4292.
E-mail address: pivovar@lanl.gov (B.S. Pivovar).

0032-3861/$ - see front matter © 2006 Elsevier Ltd. All rights reserved.
doi:10.1016/j.polymer.2006.02.032

polymer electrolytes properties, and their impact on the observed fuel cell performance.

As mentioned earlier, acid content (IEC, equivalent weight or degree of (di)sulfonation) is the chemical effect that has been the most highly reported. We begin by presenting the effect of disulfonation level within the polymers studied and relating observed behavior to that in the literature. We then move to the effects of fluorine incorporation in the copolymer backbone. The effect of fluorination is a subject that has been presented in comparative studies between perfluorosulfonic acid and hydrocarbon copolymers [13,14], but not within similar polymer families at varying degrees of fluorination as presented here. The other structural variable investigated is polar group incorporation. Polar groups have been previously investigated due to their exceptional ability to disperse highly conductive inorganic additives [15,16]. In this paper, we focus on the effect of polar group on observed properties without the incorporation of additives.

As a baseline material, we chose biphenol-based disulfonated polysulfones (BP). In order to introduce fluorine moiety, the biphenol monomer was replaced with hexafluoro (6F) bisphenol A. This partially substituted system can serve as a link between perfluorosulfonic acid (wholly-fluorinated) and wholly aromatic hydrocarbon copolymers (non-fluorinated). For polar group incorporation, the diphenylsulfone monomer was replaced with either benzonitrile or tri-phenyl phosphine oxide (PPO). Because these polymers are made from disulfonated monomers, disulfonation level can be modified independently within any given family. These substitution patterns have allowed us to systematically investigate the role of acid, fluorine and polar group incorporation on structure–property–performance relationships.

Among fuel cell related properties, we primarily focus on water uptake, number of water molecules per sulfonic acid site, proton conductivity and methanol permeability drawing comparisons between polymers of similar IEC. Other important factors such as morphology and the state of water within the polymer are also discussed based on previously reported studies. Finally, these properties are related to PEM fuel cell performance and discussed with aspects of molecular design and application of future generation polymer electrolytes in mind.

2. Experimental

Fig. 1 shows the chemical structure and sample code for the protonated form of disulfonated poly(arylene ether) copolymers used in this study. All copolymers used in this study were kindly supplied by the research group of Prof James McGrath at Virginia Polytechnic and State University, where the copolymers were synthesized by nucleophilic substitution polycondensation of sulfonated aromatic dihalides, one of three aromatic dihalides and one of two structurally distinct bisphenols, i.e. 4,4′-biphenol and hexafluoro bisphenol A in *N*-methylpyrrolidionone (NMP) or *N*,*N*-dimethylacetamide [17–22]. This direct copolymerization gave precise control

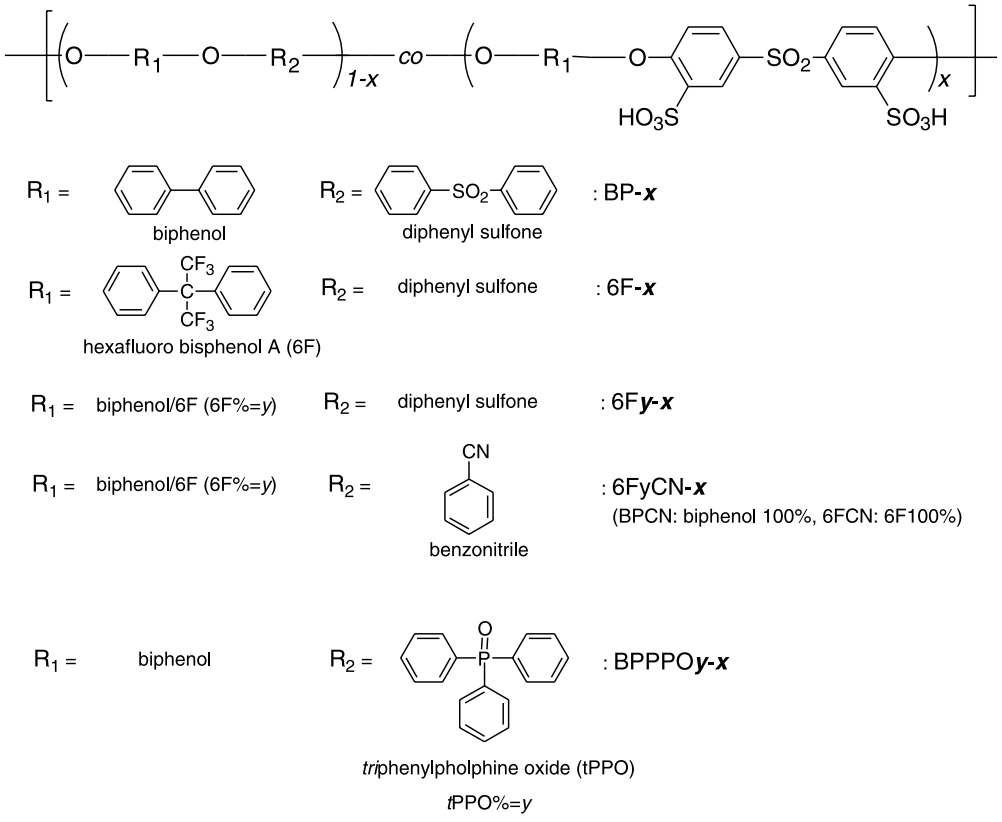

Fig. 1. Chemical structure of disulfonated poly(arylene ether sulfone) copolymers where the letter *x* in abbreviation refers to the sulfonation percentage of a disulfonated monomer.

over degree of disulfonation with random copolymerization due to ether–ether exchange reactions. Since the synthesized polysulfones were initially in the potassium sulfonate form, they were converted into acid from by the boiling of cast membranes in 0.5 M sulfuric acid for 1.5 h, followed by 1.5 h of excess acid extraction in boiling deionized water [23]. Intrinsic viscosity of these copolymers was in the range of 1.2–1.6 dL/g in NMP at 30 °C, and generally increased with IEC (or degree of disulfonation) and molecular weight. The relative molecular weight of these copolymers was in the range of 25,000–50,000 g/mol by GPC.

Water uptake (WU)was measured after drying the membrane in acid form at 100 °C under vacuum overnight. The dried membrane was immersed in water at 30 °C and periodically weighed on an analytical balance until a constant water uptake weight was obtained. The weight and volume based water uptake is reported as a percentage using the following equations

$$\text{WU (mass\%)} = (W_{\text{wet}} - W_{\text{dry}})/W_{\text{dry}} \times 100,$$

$$\text{(WU) (vol\%)} = ((W_{\text{wet}} - W_{\text{dry}})/\delta_{\text{w}})/(W_{\text{dry}}/\delta_m) \times 100$$

where W_{wet} and W_{dry} are the weights of the wet and dry membranes, respectively; δ_m is the membrane density in the dry state, and δ_{w} is the density of water (lg/cm^3).

Due to the molecular weight variation of monomer building blocks, the IEC of different copolymers changed even at the same degree of disulfonation. We calculated a weight based IEC (IEC_{W}) from the copolymer structure, which were typically 5–10% higher than the experimental value measured from non-aqueous potentiometric titration [19,20]. The typical range of IEC_{W} studied was 1.12–1.87 mequiv./g. All IEC_{W} are reported on the basis of the dry polymer. Copolymer density was measured from a known membrane dimension and weight after drying at 75 °C for 2 h. A volume based IEC (IEC_{V}) was then obtained by multiplying the membrane density to IEC_{W}. This calculation resulted in IEC_{V} (dry) based on the dry membrane density. An IEC_{V} (wet) was then also calculated based on water uptake measurements using the following equation:

$$\text{IEC}_{\text{V}}(\text{wet}) = \text{IEC}_{\text{V}}(\text{dry})/(1 + 0.01\text{WU})$$

The data are presented in terms of each IEC, and the importance of each is discussed in detail later. All membranes, cast from dimethlyacetamide solution (10% w/v), were transparent and had favorable tough/ductile characteristics, durable over several thousand hours under fuel cell conditions [24].

Proton conductivity was measured using a Solatron 1260 impedance analyzer over the frequency range of 10 Hz–1 MHz, using a reported procedure [19].

Membrane electrode assemblies (MEAs) were prepared for fuel cell testing from cast membranes. MEAs were prepared from standard catalyst inks using unsupported Pt–Ru catalyst for anode and Pt catalyst for cathode following protocols from our laboratory [25]. The geometric active cell area was 5 cm^2. The anode and cathode catalyst loading was approximately 10 and 6 mg/cm^2, respectively.

Limiting methanol crossover currents through the membrane in a cell were measured to estimate methanol permeability. For the data reported here, 0.5 M methanol solution was fed to one side of the 5 cm^2 cell, while humidified nitrogen at 500 sccm and ambient pressure was supplied to the other side. The methanol permeation flux was determined from the limiting current density resulting from transport-controlled methanol electro-oxidation at the other side of the cell using a potential step experiment [26]. Methanol permeability was calculated from following equation

$$\text{Methanol permeability (cm}^2\text{/s)} = (\xi t)/(6Fc)$$

where, ξ is the methanol crossover limiting current (A/cm^2); t is the wet membrane thickness (cm); F is the Faraday constant (s A mol); c is the methanol feed concentration (mol/cm^3).

3. Results and discussion

3.1. Effect of disulfonation level

The most common chemical variation of polymer electrolytes has been that of varying acid group content (IEC, equivalent weight or degree of (di)sulfonation). In this study, we first report fuel cell relevant properties of three classes of polymers (BP, 6F and 6FCN) as a function of disulfonation level, see Table 1. The data in Table 1 are consistent with those reported in other studies of sulfonation level within a family of copolymers [19–21]. For example, the water uptake, the number of waters per sulfonic acid site (λ), and proton conductivity all increase within a copolymer family as a function of disulfonation level (or IEC). While this data is useful for those interested in the application of specific membranes for improved fuel cell performance, these trends are very predictable and serve little interest in the investigation of chemical and structural effects. However, they do serve as an appropriate baseline for investigating the impact of fluorine and polar group incorporation discussed in the following sections.

3.2. Effect of fluorine moiety

In order to investigate the effect of fluorine moiety in sulfonated copolymers, the properties of hexafluoro bisphenol A based poly(arylene ether sulfone) (6F-*x*) and copolymers of biphenol and hexafluoro bisphenol A (6FyBP-35) were compared with those of biphenol based poly(arylene ether sulfone) (BP-*x*). Structural differences between these copolymers were shown in Fig. 1, and are as follows: 6F replaced the biphenol link of BP with 6F bisphenol A; 6FyBP-35 changed the mole ratio of 6F bisphenol A to biphenol where degree of disulfonation was fixed at 35% (for example, 6F10BP-35 is a random copolymer containing 90% of the biphenol monomer and 10% of the 6F bisphenol A). Further, complicating matters in the naming scheme used, copolymers that contain 100% of a specific monomer can be related to their partially substituted

Table 1
Effect of degree of sulfonation on density, IEC, water uptake and proton conductivity

Copolymer	Density (g/cm^3)	IEC_W (mequiv./g)	IEC_V (dry) (mequiv./cm^3)	IEC_V (wet) (mequiv./cm^3)	Water uptake (wt%)	Water uptake (vol%)	λ (H_2O/SO_3)	Proton conductivity (m S/cm)
BP-20	1.22	0.92	1.12	0.93	17	21	10.2	16
BP-25	1.26	1.11	1.40	1.09	23	29	11.5	23
BP-30	1.30	1.34	1.74	1.24	31	40	12.9	40
BP-35	1.34	1.54	2.06	1.34	40	54	14.4	72
BP-40	1.38	1.72	2.37	1.30	60	83	19.4	104
BP-45	1.41	1.92	2.74	1.15	98	138	28.4	140
6F-25	1.42	0.85	1.19	1.02	12	17	7.8	26
6F-30	1.46	1.00	1.46	1.16	18	26	10.0	38
6F-35	1.50	1.12	1.68	1.25	23	35	11.4	55
6F-40	1.54	1.30	2.02	1.37	31	48	13.2	92
6F-45	1.58	1.45	2.29	1.43	38	60	14.6	130
6FCN-20	1.30	0.82	1.07	0.99	6	8	4.1	16
6FCN-30	1.36	1.16	1.58	1.27	18	24	8.6	35
6FCN-35	1.40	1.33	1.86	1.39	24	34	10.0	58
6FCN-40	1.44	1.46	2.10	1.47	30	43	11.4	80
6FCN-45	1.46	1.61	2.35	1.54	36	53	12.4	105

analogues (for example, BP-35 and 6F-35 are equivalent to 6F0BP-35 and 6F100BP-35, respectively). In order to simplify interpretation of the data, alternative (equivalent) names for polymers are often given within tables.

Table 2 shows the density, IEC, water uptake and proton conductivity of the copolymers tested as a function of fluorination level. The only chemical differences within these copolymer families are the relative ratio of the 6F bisphenol A group to the biphenol group. While the changes observed in properties can not wholly be attributed to fluorination, due to structural differences between bisphenol A and biphenol; the system presented here was chosen because of significantly more experience with the homopolymers of BP and 6F. Additionally, we believe that the factors dominating performance reported here have more to do with fluorination than structural differences, because an earlier study of biphenol, bisphenol A and 6F bisphenol A based polymers showed modest property changes for the hydrocarbon based membranes (biphenol versus bisphenol A), but significant property changes for the partially fluorinated system (6F bisphenol A) [27]. Therefore, we feel justified presenting the observed property differences in terms of fluorine content, and believe that differences due to chemical structure are secondary in this specific comparison.

The data in Table 2 show that water uptake, λ and proton conductivity decrease in a systematic way with increasing fluorine content for both the 6F and 6FCN family of copolymers at similar disulfonation levels. However, when water uptake of these copolymers (BP-*x* and 6F-*x*, and partially substituted 6F*y*BP-35 copolymers) are plotted as a function of IEC_W (Fig. 2(a)), the data show almost no dependence on polymer chemistry, exhibit a clear trend of increasing water uptake with IEC_W, and are consistent with other directly copolymerized polysulfones having bisphenol A or hydroquinone units in the backbone [20]. These data exhibit a deflection point at 1.55 mequiv./g where water uptake increases substantially faster with IEC_W, similar to that reported for other systems in the literature and related to a percolation threshold [19,20,28].

Based on the data presented in Fig. 2(a), one might argue chemistry plays little role in water uptake. However, using IEC_W for screening polymer properties, although common, is problematic. Choosing any weight normalized quantity (IEC_W or water uptake (wt%)) as a basis for comparison adds importance to the density of the polymer and creates differences between hydrocarbon (lower density) and fluorinated (higher density) polymers based on mass that would not be expected to affect fuel cell relevant properties. While

Table 2
Effect of fluorine moiety on density, IEC, water uptake and proton conductivity

Copolymer	Density (g/cm^3)	IEC_W (mequiv./g)	IEC_V (dry) (mequiv./cm^3)	IEC_V (wet) (mequiv./cm^3)	Water uptake (wt%)	Water uptake (vol%)	λ (H_2O/SO_3)	Proton conductivity (m S/cm)
6F0-35 (BP-35)	1.34	1.54	2.06	1.34	40	54	14.4	72
6F10-35	1.34	1.43	1.93	1.30	36	48	14.0	62
6F30-35	1.37	1.34	1.84	1.28	32	44	13.3	60
6F50-35	1.42	1.27	1.80	1.27	29	41	12.7	58
6F100-35 (6F-35)	1.50	1.12	1.68	1.25	23	35	11.4	55
6F0CN-35 (BPCN-35)	1.33	1.87	2.49	1.63	40	53	11.9	78
6F25CN-35	1.34	1.70	2.29	1.55	35	47	11.4	70
6F50CN-35	1.36	1.56	2.12	1.49	31	42	11.0	65
6F75CN-35	1.40	1.44	1.98	1.41	27	38	10.4	62
6F100CN-35 (6FCN-35)	1.40	1.33	1.86	1.39	24	34	10.0	58

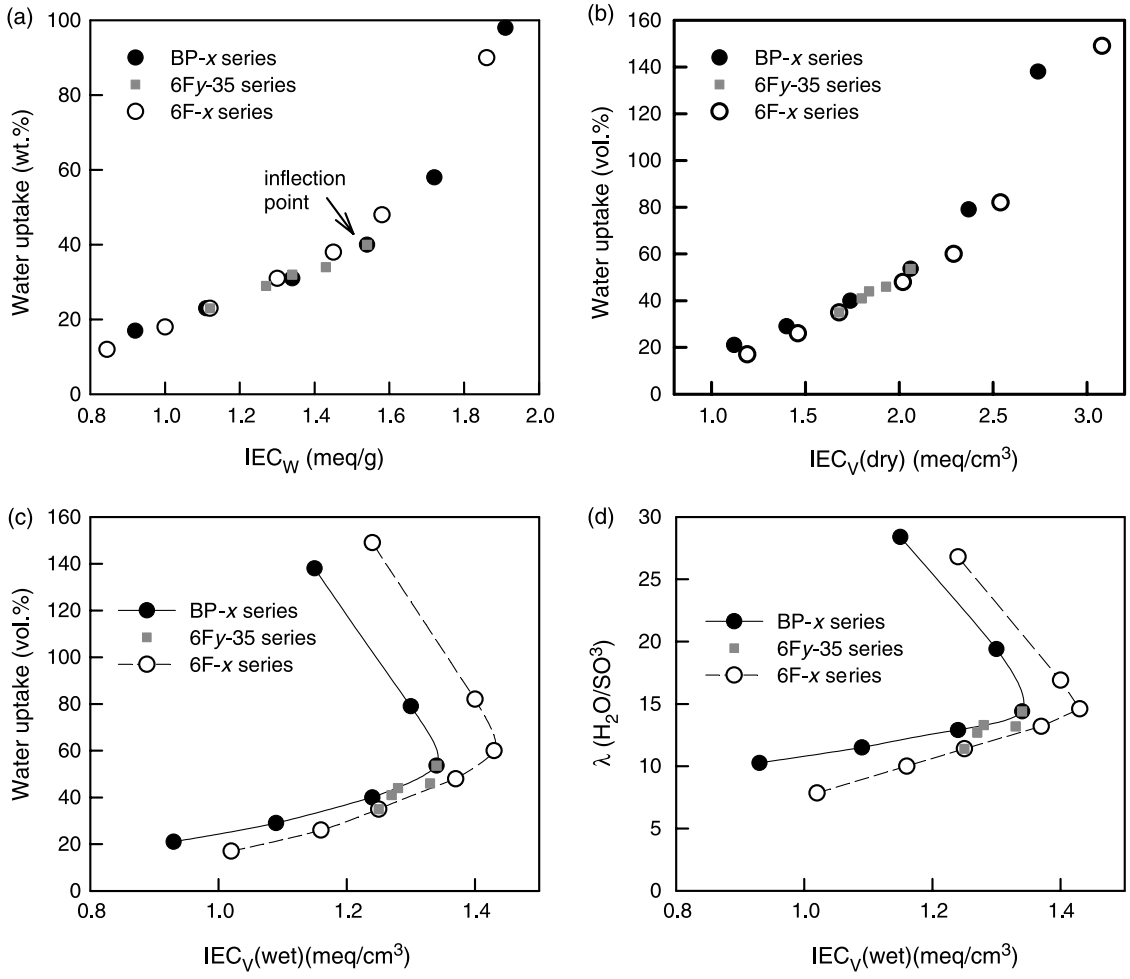

Fig. 2. Effect of fluorine incorporation on membrane water uptake as a function of (a) IEC_W, (b) IEC_V (dry), (c) IEC_V (wet), and (d) number of water molecules associated with sulfonic acid group (λ) as a function of IEC_V (wet).

polymer density does affect water uptake (wt%); in general, choosing quantities that are weighted by volume rather than mass serve a more reasonable comparison basis. This stems from the fact that changes in length scale (reflected in volume measurements) are expected to directly impact observed properties (i.e. conductivity and permeability) and changes in mass of the polymer are not.

When IEC_W is changed to IEC_V (still on a dry polymer basis—IEC_V (dry)) and water uptake (wt%) is changed to water uptake (vol%), modest changes result as shown in Fig. 2(b). The volume normalized data in Fig. 2(b) follow the same trends as the weight normalized data in Fig. 2(a), except a clear trend to slightly decreased water uptake based on fluorination is discernable between the BP and 6F polymers. Incidentally, if a weight based water uptake were used in Fig. 2(b), although still small, a larger gap between the fluorinated and non-fluorinated polymers is evident due to the lower density of the hydrocarbon membrane.

While the changes in water uptake shown in Fig. 2(b) are small, much more significant differences due to fluorination are apparent when considering IEC_V on a wet basis, see Fig. 2(c). In this case the fluorinated copolymer (6F) shows much lower water uptake at a given IEC_V (wet). Both the fluorinated and non-fluorinated copolymers exhibit an inflection point at high IEC_V (wet) where a percolation threshold is reached and substantially increased water uptake results in lowering of IEC_V (wet). Although, this inflection point happens at a much higher IEC_V (wet) for the fluorinated polymer. The controlled fluorine content 6F*y*BP-35 system shows the expected trend of tending from the non-fluorinated (BP-*x*) to fluorinated (6F-*x*) system as a function of fluorine substitution. The trends in water uptake shown in Fig. 2(c) are even larger for λ as a function of IEC_V (wet), Fig. 2(d). This is because at the same water uptake, IEC_V (wet) is much larger for the fluorinated copolymer than non-fluorinated copolymer. Fig. 2(c) and (d) show the clear importance of fluorine moieties on water uptake.

We have used IEC_V (wet) as a basis for comparison because it reflects the concentration of ions within the polymer matrix under hydrated (operationally relevant) conditions. While other aspects such as morphology and specific chemical interactions are important and will be discussed later, when considering IEC, Fig. 2 shows the clear risks of using mass normalized or dry polymer IECs as a basis for comparison. For this reason we will use IEC_V (wet) and water uptake (vol%) within the rest of this paper even though IEC_W is the most easily obtained and most often reported IEC.

While water uptake has a strong influence on fuel cell related properties, it is proton conductivity that is the property of primary importance for fuel cell applications. The effects of incorporation of fluorine moiety are also very apparent when considering proton conductivity. Fig. 3 shows the proton conductivity of the selected copolymers as a function of IEC_V. Again, significant differences result in comparing fluorinated and non-fluorinated polymers. At a given IEC_V the fluorinated system (6F) exhibited significantly higher conductivity except for disulfonation levels above the inflection point. These copolymers are of relatively little use in fuel cells as they swell significantly and have poor mechanical properties. For polymers with reasonable mechanical properties, fluorinated polymers exhibit significant advantages. The proton conductivities of the controlled fluorine content 6FyBP-35 series, like the water uptakes shown in Fig. 2, changed in a predictable, systematic fashion as the level of fluorine moiety increased.

In order to isolate the effects of fluorine moiety, data in Tables 1 and 2 was interpolated to give conductivity, water uptake and λ at a fixed IEC_V (1.28 mequiv./cm^3). The proton conductivity, water uptake and λ are reported as a function of atomic fluorine composition for different copolymers in Fig. 4. The data in Fig. 4 clearly show that conductivity increases with fluorine composition at this fixed IEC_V. Interestingly, although proton conductivity was shown to increase significantly with water uptake and λ within a family of copolymers (Table 1), the conductivity of copolymers at fixed IEC_V increased with decreasing λ and water uptake, in part due to the increasing level of disulfonation at fixed IEC_V.

Based on the data presented in Figs. 3 and 4, phase separation or morphological differences between the selected copolymers appears to be driven by fluorine incorporation. Sulfonated copolymers have hydrophilic (sulfonated) and hydrophobic (aromatic, non-sulfonated and/or fluorinated) segments, which are prone to phase separate. When hydrophobic fluorine moiety is incorporated into the copolymer backbone, it can increase the hydrophobicity of those backbone segments and induce a greater degree of phase separation

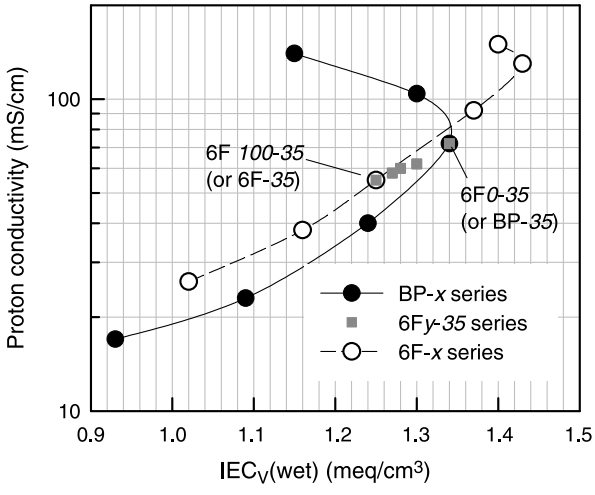

Fig. 3. Effect of fluorine incorporation on proton conductivity as a function of IEC_V (wet).

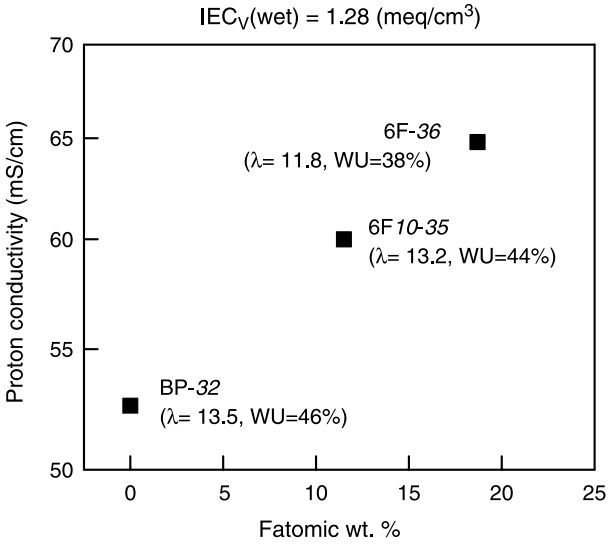

Fig. 4. Effect of fluorine incorporation on proton conductivity at a fixed IEC_V (wet).

leading to more distinct and more strongly hydrophilic/hydrophobic phases. Increased phase separation likely leads to changes in tortuosity and the state of water within these polymers, a topic reported previously in the literature for these materials [12,13,29]. These literature references also support increased phase separation with increasing fluorine content by increased free-water measurements made by differential scanning calorimetry and ^{1}H pulse nuclear magnetic resonance. Shorter conduction pathways and increased free water content due to increased phase separation are likely the driving forces behind the increased conductivity with increasing fluorine content shown in Fig. 4.

3.3. Effect of polar functional group

The effect of incorporation of two different polar groups in either the BP or 6F series: (1) benzonitrile (CN) and (2) phenyl phosphine oxide (PPO) group were explored. For benzonitrile group incorporation, the diphenylsulfone unit was completely replaced with benzontrile in the 6F series (versus 6FCN) or BP-35 (versus BPCN-35). For the PPO series diphenylsulfone was partially replaced with benzontrile for BP-35 or BP-40 (versus BPPPO*y*-35 or 40). Both benzonitrile and PPO groups are known to be strongly polar and have strong interactions with other polar groups (i.e. hydrogen bonding) [30–34]. The benzonitrile group has a large dipole moment (ca. 4.18 D) and a large polarizability, which is capable of forming a stable complex with water molecules. Hydrogen bonding with benzonitrile and its strength in the presence of water molecules has been detected and measured by various analytical tools such as microwave, high-resolution UV and infrared spectroscopy [30,31]. These studies indicate that water molecules bind to benzonitrile from the side, in-plain to the aromatic ring via two hydrogen bonds. The PPO group, on the other hand, is known to exhibit strong hydrogen bonding with other

Table 3
Effect of polar group on density, IEC, water uptake and proton conductivity

Copolymer	Density (g/cm^3)	IEC_W (mequiv./g)	IEC_V (dry) (mequiv./cm^3)	IEC_V (wet) (mequiv./cm^3)	Water uptake (wt%)	Water uptake (vol%)	λ (H_2O/SO_3)	Proton conductivity (m S/cm)
BP-35	1.34	1.54	2.06	1.34	40	54	14.4	72
BPCN-35 (6F0CN-35)	1.33	1.87	2.49	1.63	40	53	11.9	78
6F-30	1.46	1.00	1.46	1.16	18	26	10.0	38
6FCN-30	1.36	1.16	1.58	1.27	18	24	8.6	35
6F-35	1.50	1.12	1.68	1.25	23	35	11.4	55
6FCN-35	1.40	1.33	1.82	1.39	24	34	10.0	58
6F-40	1.54	1.30	2.02	1.37	31	48	13.2	92
6FCN-40	1.44	1.46	2.10	1.47	30	43	11.4	80
6F-45	1.58	1.45	2.29	1.43	38	60	14.6	130
6FCN-45	1.46	1.61	2.35	1.54	36	53	12.4	105
BPPPO0-35 (BP-35)	1.34	1.54	2.06	1.34	40	54	14.4	72
BPPPO30-35	1.35	1.40	1.89	1.40	26	35	10.3	35
BPPPO0-40 (BP-40)	1.38	1.72	2.37	1.30	60	83	19.4	104
BPPPO30-40	1.25	1.57	1.97	1.39	33	41	11.7	38
BPPPO40-40	1.19	1.56	1.87	1.42	27	32	9.6	29
BPPPO50-40	1.16	1.55	1.80	1.42	23	27	8.2	21

functional groups including hydroxyl [32], imide [33], and sulfonic and phosphoric acid [34].

The density, IEC, water uptake, λ, and proton conductivity for selected copolymers as a function of polar group incorporation are summarized in Table 3. The data for water uptake are shown in Fig. 5(a) and (b) as a function of IEC_V for benzonitrile and PPO containing copolymers, respectively. In comparing benzonitrile containing polymers (6FCN) to analogous polymers without benzonitrile (6F), water uptake was found to decrease in a significant manner ($\sim$25%) at any given IEC_V for the benzonitrile containing polymers. BPPPO*y* also showed lower water uptake than the non-functionalized system (i.e. BP) and the degree of decreasing water uptake was more significant with higher PPO composition. These results indicate that polar groups such as benzonitrile and PPO play a significant role in reducing water uptake. This observation is consistent with other copolymers having specific interactions that suppress membrane swelling under hydrating conditions.

The proton conductivity of these copolymers as a function of IEC_V is shown in Fig. 6. Almost immediately apparent is the similarity between Figs. 5 and 6. The qualitative similarity between Figs. 5 and 6 is a reflection of the role of water on proton conduction in these copolymers. Proton transport in polymer electrolytes relies on water to ionize acid sites and provide mobility (conductivity) for the proton. For the two polar groups investigated here, it appears that their primary impact is in preventing water uptake.

These effects are isolated in Fig. 7 where the effects of PPO group incorporation at roughly the same IEC_V ($\sim$1.4 mequiv./cm^3) are plotted as a function of proton conductivity. Values of water uptake (WU) and λ have been added to Fig. 7 in order to discuss trends. There is a clear trend in this data toward decreasing conductivity with increasing PPO group incorporation. The water uptake and λ of these polymers also decrease with increasing PPO content. While these trends are

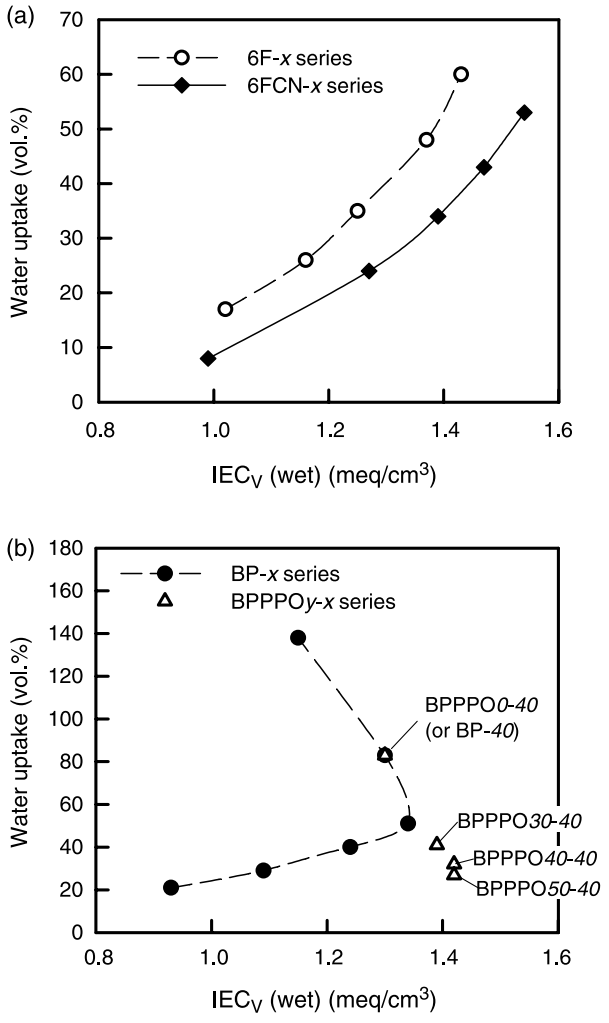

Fig. 5. Effect of (a) benzonitrile and (b) PPO polar group incorporation on membrane water uptake.

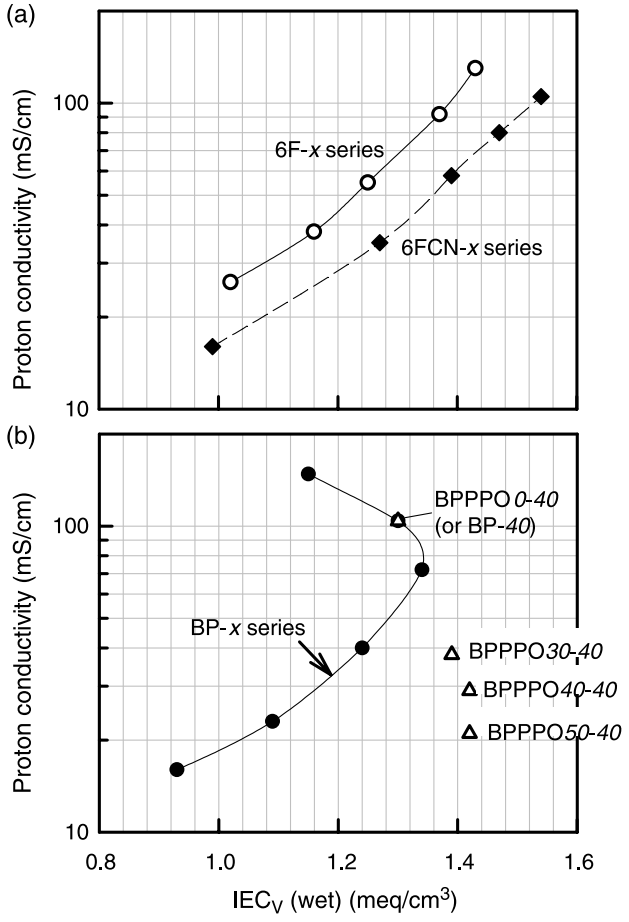

Fig. 6. Effect of (a) benzonitrile and (b) PPO polar group incorporation on membrane proton conductivity.

unsurprising as they have been shown for many polymer electrolytes as a function of sulfonation level (such as those shown in Table 1); they run counter to those reported in Fig. 4 for the effects of fluorine incorporation. Whereas, fluorine incorporation exhibited trends suggesting increased phase separation, the data for PPO group incorporation suggest its primary role is that of water exclusion, although specific interactions with other polymeric moieties like sulfonic acid cannot be ruled out based on this data. Interestingly, Roy et al. demonstrated that PPO containing polysulfones had higher free water fraction compared to BP control using pressurized DSC and pulse field gradient NMR experiments [35]. This result is surprising due to the lower water uptake of the PPO containing polysulfones and suggests that the role of PPO within the polymer framework is more complicated than simple water exclusion and its specific interactions are also important.

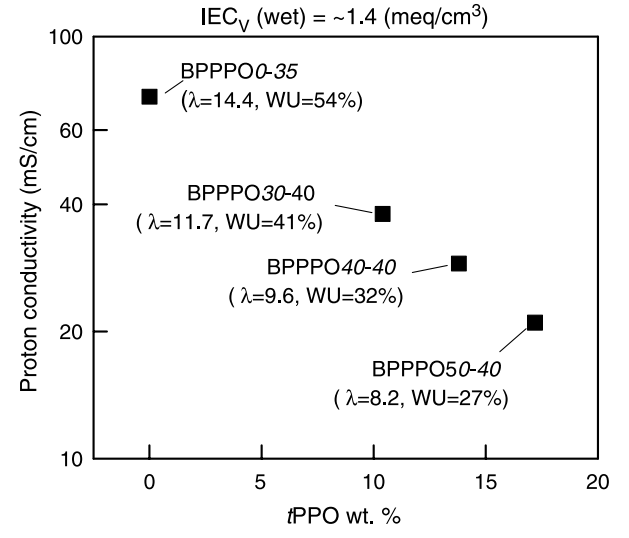

Fig. 7. Effect of PPO incorporation on proton conductivity at a fixed IEC_V (wet).

While decreasing conductivity is a shortcoming of polar group incorporation, polar group incorporation may lead to advantages in mechanical properties, decreased membrane–electrode interfacial resistance or in direct methanol fuel cells (DMFCs) due to decreased methanol crossover. Methanol permeability is directly related to methanol crossover, and selectivity (the ratio of proton conductivity to methanol permeability) has been put forward as a qualitative basis for evaluating the potential of a polymer as an electrolyte in DMFCs [36]. Table 4 contains data for the proton conductivity, methanol permeability and selectivity of selected copolymers at different degrees of polar group incorporation. Nafion has been added to Table 4 for comparison purposes because it is the standard membrane used in DMFCs, in spite of its poor selectivity. For the polymers listed in Table 4, all have lower conductivity than Nafion. However, methanol permeability of these other copolymers is also significantly decreased, resulting in better selectivity for each of the alternative polymers presented. In comparing the effects of polar group incorporation, it is apparent that PPO incorporation although significantly lowering methanol permeability offers no improvement in selectivity compared to the base BP copolymers. The incorporation of benzonitrile, on the other hand, leads to the most selective copolymer (BPCN-35) presented in Table 4. Both the fluorinated (6F) and non-fluorinated polymers (BP) show increases in selectivity with benzonitrile incorporation. The addition of PPO or benzonitrile in these systems of polymers has significantly different effects and shows the importance of not only polar character, but the nature of interactions with specific polar groups.

Table 4
Methanol permeability and selectivity of selected copolymers

Copolymer	*t*PPO (or benzonitrile) content (wt%)	Proton conductivity (m S/cm)	Methanol permeability ($\times 10^6$) (cm^2/s)	Selectivity ($\times 10^{-2}$) (S m/s)
BPPPO50-40	17.2	21	0.55	3.8
BPPPO40-40	13.8	29	0.67	4.3
BPPPO30-35	12.4	35	0.82	4.3
BPPPO30-40	10.5	38	1.02	3.7
BPCN-35	(17.2)	78	1.44	5.4
6FCN-35	(14.1)	58	1.32	3.6
6F-35	0	55	1.66	3.3
BP-35	0	72	1.55	4.7
BP-40	0	104	2.20	4.7
Nafion	0	111	4.20	2.6

It is worth noting that the incorporation of fluorine moiety into the copolymer backbone, although found to be advantageous for proton conduction, results in lower selectivity as shown in Table 4. This result is in agreement with increased phase separation proposed during our discussion of the effect of fluorine incorporation.

3.4. Impact on fuel cell performance

The final step required in drawing a link between structure, property and performance within these copolymers is to evaluate fuel cell performance. It is straightforward that higher membrane conductivity reduces the ohmic resistance of fuel cells and thus improves performance. Fig. 8 compares the H_2/air fuel cell performance of structure-modified membranes at similar IEC_V and membrane thickness. The fuel cells were operated under identical conditions (i.e. cell temperature, catalyst loading, reactant stoichiometry, back pressure, etc.). Fig. 8(a) shows that 6F exhibits superior performance due to decreased ohmic losses reflected in its lower high frequency resistance (HFR) compared to the BP control. The HFR for BP was 153 mΩ cm^2 which was approximately 25% higher than that of 6F counterpart (123 mΩ cm^2). This HFR difference qualitatively agreed well with the free-standing membrane conductivity reported in Table 1. Fig. 8(b) compares a PPO

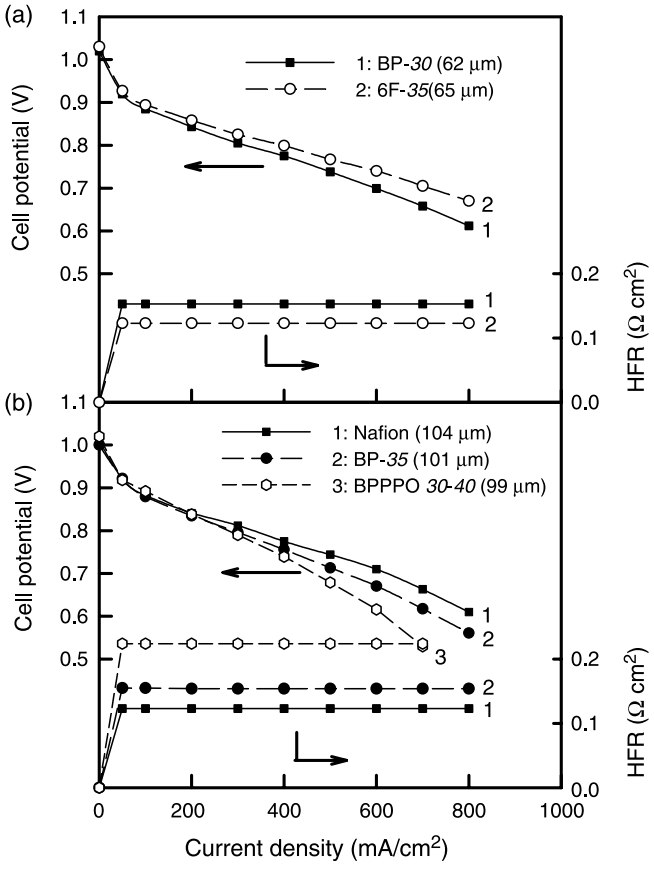

Fig. 8. Effect of (a) fluorine and (b) PPO incorporations on H_2/air fuel cell performance at 80 °C; IEC_V (wet) values of membranes for (a) and (b) were fixed at 1.25 and 1.35 mequiv./cm^3, respectively.

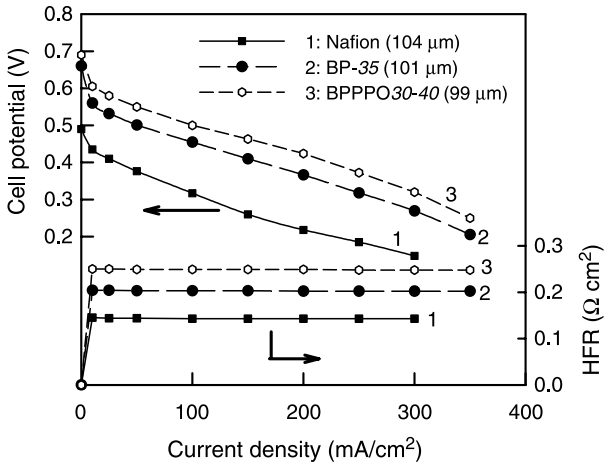

Fig. 9. Effect of PPO incorporations on high methanol concentration feed (5 M) DMFC performance at 80 °C; IEC_V (wet) value of membranes was fixed at 1.35 mequiv./cm^3.

containing membrane with a BP and Nafion control. The BPPPO membrane had a higher HFR and thus poorer performance than BP control. For hydrogen fuel cells, one could conclude that fluorine incorporation gives an advantageous effect while PPO group incorporation adversely impacted fuel cell performance due to changes in proton conductivity.

Thus far, we have focused only on conductivity and not on aspects of mechanical robustness or membrane–electrode interfacial compatibility. While membrane conductivity (or lower cell resistance) increases with IEC, increasing IEC is usually accompanied by greater membrane water uptake. Higher water uptake results in poorer mechanical properties and potential electrode compatibility issues. Previous research indicated that increased water uptake of membrane resulted in increased membrane–electrode interfacial delamination and significant performance degradation [37,38]. In these regards, we could expect advantages from both fluorine and polar group incorporation.

Additionally, the copolymers presented demonstrate improved selectivity compared to Nafion and would be expected to be better electrolytes in DMFCs. This is particularly true at high methanol feed concentrations (> 2 M) where the effects of methanol crossover are amplified. Fig. 9 demonstrates DMFC performance of BPPPO30-40, BP-35 and Nafion at a 5 M methanol feed concentration. Although the cell resistance of BPPPO30-40 was much greater than BP-35 and Nafion, the fuel cell performance of BPPPO30-40 was superior. This result reflects the fact that copolymers having polar group incorporation can significantly suppress methanol transport, of particular use in high methanol feed concentration DMFCs. Further efforts in tailoring sulfonated polysulfone properties using fluorine and polar group moieties are being pursued [39].

4. Conclusions

Structure–property–performance relationships of directly copolymerized poly(arylene ether sufone) were investigated.

The polysulfone membrane incorporated with hexafluoro bisphenol A (6F) showed decreased water uptake compared to non-fluorinated polysulfones (BP) while conductivity increased at a similar IEC, attributed to a greater degree of phase separation. The polysulfone membranes incorporated with polar groups such as benzonitrile and PPO, on the other hand, showed decreased water uptake, conductivity and methanol permeability. Increased conductivity of the fluorine incorporated system improved fuel cell performance by reducing cell resistance, while polar group incorporation adversely impacted the fuel cell performance by lowering conductivity. Improvements in selectivity and DMFC performance, at high methanol feed concentration, were shown for all alternative copolymers tested.

Acknowledgements

Expressed appreciation to the US Department of Energy and the Defense Advanced Research Project Agency (DARPA) for support. Research group of Drs James E. McGrath and Judy Riffle (Virginia Polytechnic and State University) for supply of polysulfone copolymers.

References

[1] Savadogo O. J New Mater Electrochem Syst 1998;1:47.
[2] Roziere J, Jones DJ. Ann Rev Mater Res 2003;33:503.
[3] Hickner M, Ghassemi H, Kim YS, Einsla B, McGrath JE. Chem Rev 2004;104:4587–612.
[4] Zaidi SMJ, Mikhailenko SD, Robertson GP, Guiver MD, Kaliaguine S. J Membr Sci 2000;173:17.
[5] Kim YS, Dong L, Hickner MA, Pivovar BS, McGrath JE. Polymer 2003; 44:5729.
[6] Elabd YA, Napadensky E, Sloan JM, Crawford DM, Walker CW. J Membr Sci 2003;217:227.
[7] Kerres J, Ullrich A, Meier F, Haring T. Solid State Ionics 1999;125:243.
[8] Kerres J, Ullrich A, Haring T, Baldauf M, Gebhardt U, Preidel W. J New Mater Electrochem Syst 2000;3:229.
[9] Litt MH, Zhang Y, Savinell RF, Wainright JS. Polym Prepr 1999;40:480.
[10] Miyatake K, Zhou H, Uchida H, Watanabe M. Chem Commun 2003;3: 368.
[11] Xing PX, Robertson GP, Guiver MD, Mikhaileuko SD, Kaliaguine S. Macromolecules 2004;37:7960.
[12] Hickner M, Pivovar BS. Fuel Cells 2005;5:213.
[13] Kreuer KD. J Membr Sci 2001;185:29–39.
[14] Alberti G, Casciola M, Massinelli L, Bauer B. J Membr Sci 2001;185:73.
[15] Wang S, Zhuang H, Sankarapandian M, Shobha HK, Ji Q, Shultz AR, et al. Polym Prepr 2000;41:1350.
[16] Hill M, Einsla BR, Kim YS, McGrath JE. Division of fuel chemistry 228th ACS national meeting, Philadelphia, PA; 2004.
[17] Shobha HK, Smalley GR, Sankarapandian M, McGrath JE. Polym Prepr 2000;41:180.
[18] Wang F, Hickner M, Ji Q, Harrison W, Mecham J, Zawodzinski TA, et al. Macromol Symp 2001;175:387.
[19] Wang F, Hickner M, Kim YS, Zawodzinski TA, McGrath JE. J Membr Sci 2002;197:231.
[20] Harrison WL, Wang F, Mecham J, Bhanu V, Hill M, Kim YS, et al. J Polym Sci, Part A: Polym Chem 2003;41:2264.
[21] Sumner MJ, Harrison WL, Weyers RM, Kim YS, McGrath JE, Riffle JS, et al. J Membr Sci 2004;239:199.
[22] Harrison W, Hickner M, Kim YS, McGrath JE. Fuel Cells 2005;5:201.
[23] Kim YS, Wang F, Hickner M, McCartney S, Hong YT, Zawodzinski TA, et al. J Polym Sci, Part B: Polym Phys 2003;41:2816.
[24] Kim YS, Pivovar BS. Advances in materials for proton exchange membrane fuel cell systems. Abs. No 35, Pacific Grove, CA, February 20–23; 2005.
[25] Thomas SC, Ren XM, Gottesfeld S, Zelenay P. Electrochimica Acta 2002;47(22):3741.
[26] Ren X, Springer TE, Gottesfeld S. J Electrochem Soc 2000;147:92.
[27] Harrison WL, Wang F, Hickner MA, Kim YS, Hill M, Zawodzinski TA, et al. manuscript submitted in polymer.
[28] Einsla BR, Kim YS, Hickner MA, Hong YT, Hill ML, Pivovar BS, et al. J Membr Sci 2005;255:141.
[29] Kim YS, Dong L, Hickner M, Glass TE, McGrath JE. Macromolecules 2003;36(17):6281.
[30] Brutschy B. Chem Rev 2000;100:3891.
[31] Kryachko ES, Nguyen MT. J Chem Phys 2001;115:833.
[32] Wang S, Zhuang H, Shobha HK, Glass TE, Sankarapandian M, Ji Q, et al. Macromolecules 2001;34:8051.
[33] Etter MC, Reutzel SM. J Am Chem Soc 1991;113:2586.
[34] Langner R, Zundel G. J Phys Chem 1995;99:12214.
[35] Roy A, Hickner M, Glass T, McGrath JE. Advances in materials for proton exchange membrane fuel cell systems. Abs. No 55-II, Pacific Grove, CA, February 20–23; 2005.
[36] Pivovar BS, Wang Y, Cussler EL. J Membr Sci 1999;154:155.
[37] Kim YS, Pivovar BS, Abstract 1073, The Electrochemical Society Meeting Abstracts, Orlando, FL, October 12–16, 2003. Manuscript submitted in J Electrochem Soc.
[38] Kim YS, Pivovar BS, Manuscript submitted in Advances in Fuel Cells (Ed. TS Zhao), Elsevier, Oxford.
[39] Kim YS, Sumner MJ, Harrison WL, Riffle JS, McGrath JE, Pivovar BS. J Electrochem Soc 2004;151:A2150.